PERGAMON

International Journal of Heat and Mass Transfer 46 (2003) 577–587

International Journal of HEAT and MASS TRANSFER

www.elsevier.com/locate/ijhmt

Transient behaviors of ignition of premixed stagnation-point flows with catalytic reactions

W.J. Sheu *, C.J. Sun

Department of Power Mechanical Engineering, National Tsing Hua University, Hsinchu, Taiwan

Received 10 March 2002; received in revised form 9 August 2002

Abstract

Transient ignition process of premixed stagnation-point flows over a catalytic surface of a solid plate with a finite thickness is investigated numerically in this work. The results reveal that the thermal runaway criterion instead of the zero-gradient criterion is preferred for the problem of interest. Depending on system parameters, both the ignition delay and the critical rate of catalytic reactions at ignition are either conductively or catalytically controlled. The effects of catalytic reactions on ignition are positive and negative for catalytically and conductively controlled ignition mechanisms, respectively. According to these two ignition mechanisms, the qualitative and quantitative results of the ignition delay and the critical rate of catalytic reactions at ignition are systematically analyzed. In particular, the minimum ignition delay and the C-shaped ignition curve are discussed.

1. Introduction

Transient ignition process of the premixed combustible gas in stagnation-point flows over a catalytic plate with a finite thickness is investigated numerically. For a transient approach to ignition, a relevant question to ask frequently is how long it will take to ignite the mixture rather than whether the combustible mixture is ignitable or not.

The ignition criteria for various flow systems were analyzed in detail [1–20]. However, these ignition criteria were obtained according to the steady-state model. The analysis of ignition delay was absent. The minimum wall temperature at ignition instead of ignition delay was predicted. The steady ignition criteria were frequently identical with the zero-gradient criterion because the expression of $\partial T_g/\partial y = 0$ at wall was derived by the steady ignition criteria. Physically, the chemical reaction near the wall is self-sustaining according to the zero-gradient criterion because no more heat from the hot wall is needed in the gas phase. Strictly speaking, this self-sustaining state is not equivalent to the thermal runaway state which is followed by flame propagation. The thermal runaway criterion implies that a premixed flame will be established subsequently when the maximum temperature of gaseous mixture rises rapidly and then gradually levels off. Obviously, the problem of ignition delay is intrinsically unsteady such that a transient model of ignition should be adopted. Except the ignition delay of fuel droplet and solid propellant, few investigations of ignition delay have been made before [21–25] even though some flow configurations are of interest and importance, e.g., the stagnation-point flow, flat-plate boundary-layer flow, etc. Compared with the systematical results of steady ignition criteria, the theoretical investigation of ignition delay of combustible flows was inadequate. The physical concepts of ignition delay not only are of academic interest but also are frequently used in industrial ignition designs. Therefore, a transient model of ignition associated with various ignition criteria is adopted to determine the ignition delay in the present work. Both the qualitative and the quantitative comparisons between the ignition delay obtained by the zero-gradient criterion and that obtained by the thermal runaway criterion are made. These comparisons indicate whether the zero-gradient criterion

* Corresponding author. Tel.: +886-3-5715131; fax: +886-3-5722840.

E-mail address: wjsheu@mx.nthu.edu.tw (W.J. Sheu).

0017-9310/03/$ - see front matter
PII: S0017-9310(02)00344-7

Nomenclature

a_P	defined in Eq. (14)
a_L	$= \tilde{l}_t/\tilde{L}$
a_S	$= a_L^2\alpha_S$
B	frequency factor
c_P	specific heat at constant pressure
D	mass diffusivity
E	activation energy
F	defined in Eq. (26)
H	defined in Eq. (26)
L	thickness of plate
Le	Lewis number
l_t	characteristic flame thickness
n	total reaction order
n_i	reaction order
P	pressure
Pr	Prandtl number
q	specific heat of combustion
R	gas constant
R_u	universal gas constant
s_f	propagation speed of premixed flame
T	temperature
t	time
u	velocity in the x direction
v	velocity in the y direction
W	molecular weight
x	coordinate along the wall
Y	mass fraction
y	coordinate normal to the wall

Greek symbols

α	thermal diffusivity
β	temperature exponent
γ	strain rate of flow
θ	non-dimensional activation energy
λ	thermal conductivity
μ	viscosity
ν	stoichiometric coefficient
ρ	density
ω	specific reaction rate

Subscripts

c	critical value
cat	catalytic reaction at wall
F	fuel
g	gas phase
i	index for species
ig	ignition
int	interface between gas phase and solid phase
L	lower surface of plate
min	minimum value
O	oxidizer
s	solid phase
∞	cold outer flow

Superscripts

l	lower limit
o	non-catalytic limit
u	upper limit
I	first stage of ignition delay
II	second stage of ignition delay
$\sim$	dimensional or original quantities

is invalid qualitatively and quantitatively for the problem of interest. The similar comparisons have recently been made for the ignition delay of non-premixed stagnation-point flows [25]. As a counterpart, the comparisons of ignition delay of premixed stagnation-point flows with catalytic reactions according to these two types of ignition criteria are made in this work.

For the ignition with catalytic reactions, the critical rate of catalytic reactions at ignition is also of fundamental and practical interest. Conventionally, the critical rates of catalytic reactions at ignition were predicted according to steady-state models in several research works. Therefore, the previous results of critical rates of catalytic reactions at ignition [17] were not sufficient conditions for ignition from a viewpoint of the establishment of flame propagation. The subsequent flame propagation is not guaranteed according to the zero-gradient criterion adopted in steady-state models. With a transient model of ignition, the critical rate of catalytic reactions at ignition is determined here by the thermal runaway criterion instead of the zero-gradient criterion. The dependence of the critical rate of catalytic reactions at ignition on system parameters is discussed. The relevant findings extend the previous concepts of the critical rate of catalytic reactions at ignition derived by the steady ignition criteria.

2. Formulation

For the problem of interest, the following assumptions are made. The flow is unsteady, two-dimensional and laminar viscous flow; the specific heats at constant pressure of the various species are equal to a constant; the radiative heat transfer, Soret and Dufour effects are neglected; chemical reactions between the fuel (F) and the oxidizer (O) are represented by a global one-step irreversible reaction such as $F + \nu_O O \rightarrow$ products; the combustible gas is a mixture of ideal gases with constant values of $\tilde{\rho}_g\tilde{\mu}$, $\tilde{\rho}_g\tilde{\lambda}_g$ and $\tilde{\rho}_g^2\tilde{D}_i$.

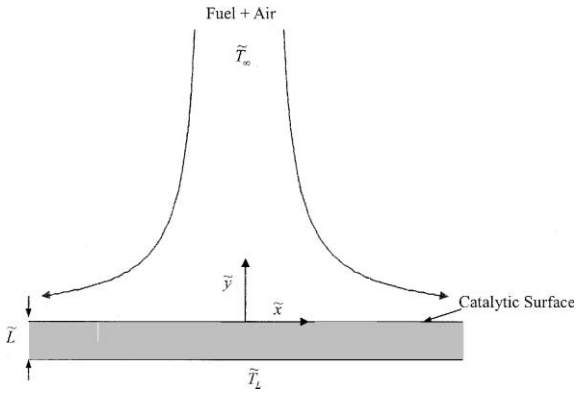

Fig. 1. Schematic of premixed stagnation-point flows over a catalytic surface of a solid plate with a finite thickness.

The physical model in the present work is a premixed stagnation-point flow over a plate with a finite thickness, as shown in Fig. 1. The catalytic reactions proceed at the upper surface of plate. With the above assumptions, the appropriate governing equations are

gas phase:

$$\frac{\partial\tilde{\rho}_g}{\partial\tilde{t}}+\frac{\partial\left(\tilde{\rho}_g\tilde{u}\right)}{\partial\tilde{x}}+\frac{\partial\left(\tilde{\rho}_g\tilde{v}\right)}{\partial\tilde{y}}=0 \tag{1}$$

$$\tilde{\rho}_g\left(\frac{\partial\tilde{u}}{\partial\tilde{t}}+\tilde{u}\frac{\partial\tilde{u}}{\partial\tilde{x}}+\tilde{v}\frac{\partial\tilde{u}}{\partial\tilde{y}}\right)=-\frac{\partial\tilde{P}}{\partial\tilde{x}}+\frac{\partial}{\partial\tilde{y}}\left[\tilde{\mu}\left(\frac{\partial\tilde{u}}{\partial\tilde{y}}+\frac{\partial\tilde{v}}{\partial\tilde{x}}\right)\right]+\frac{\partial}{\partial\tilde{x}}\left(2\tilde{\mu}\frac{\partial\tilde{u}}{\partial\tilde{x}}\right)-\frac{\partial}{\partial\tilde{x}}\left[\frac{2}{3}\tilde{\mu}\left(\frac{\partial\tilde{u}}{\partial\tilde{x}}+\frac{\partial\tilde{v}}{\partial\tilde{y}}\right)\right] \tag{2}$$

$$\tilde{\rho}_g\left(\frac{\partial\tilde{v}}{\partial\tilde{t}}+\tilde{u}\frac{\partial\tilde{v}}{\partial\tilde{x}}+\tilde{v}\frac{\partial\tilde{v}}{\partial\tilde{y}}\right)=-\frac{\partial\tilde{P}}{\partial\tilde{y}}+\frac{\partial}{\partial\tilde{x}}\left[\tilde{\mu}\left(\frac{\partial\tilde{u}}{\partial\tilde{y}}+\frac{\partial\tilde{v}}{\partial\tilde{x}}\right)\right]+\frac{\partial}{\partial\tilde{y}}\left(2\tilde{\mu}\frac{\partial\tilde{v}}{\partial\tilde{y}}\right)-\frac{\partial}{\partial\tilde{y}}\left[\frac{2}{3}\tilde{\mu}\left(\frac{\partial\tilde{u}}{\partial\tilde{x}}+\frac{\partial\tilde{v}}{\partial\tilde{y}}\right)\right] \tag{3}$$

$$\tilde{\rho}_g\tilde{c}_{P,g}\left(\frac{\partial\widetilde{T}_g}{\partial\tilde{t}}+\tilde{u}\frac{\partial\widetilde{T}_g}{\partial\tilde{x}}+\tilde{v}\frac{\partial\widetilde{T}_g}{\partial\tilde{y}}\right)=\frac{\partial}{\partial\tilde{x}}\left(\tilde{\lambda}_g\frac{\partial\widetilde{T}_g}{\partial\tilde{x}}\right)+\frac{\partial}{\partial\tilde{y}}\left(\tilde{\lambda}_g\frac{\partial\widetilde{T}_g}{\partial\tilde{y}}\right)+\tilde{q}\tilde{W}_F\tilde{\omega}_g \tag{4}$$

$$\tilde{\rho}_g\left(\frac{\partial\widetilde{Y}_F}{\partial\tilde{t}}+\tilde{u}\frac{\partial\widetilde{Y}_F}{\partial\tilde{x}}+\tilde{v}\frac{\partial\widetilde{Y}_F}{\partial\tilde{y}}\right)=\frac{\partial}{\partial\tilde{x}}\left(\tilde{\rho}_g\widetilde{D}_F\frac{\partial\widetilde{Y}_F}{\partial\tilde{x}}\right)+\frac{\partial}{\partial\tilde{y}}\left(\tilde{\rho}_g\widetilde{D}_F\frac{\partial\widetilde{Y}_F}{\partial\tilde{y}}\right)-\tilde{W}_F\tilde{\omega}_g \tag{5}$$

$$\tilde{\rho}_g\left(\frac{\partial\widetilde{Y}_O}{\partial\tilde{t}}+\tilde{u}\frac{\partial\widetilde{Y}_O}{\partial\tilde{x}}+\tilde{v}\frac{\partial\widetilde{Y}_O}{\partial\tilde{y}}\right)=\frac{\partial}{\partial\tilde{x}}\left(\tilde{\rho}_g\widetilde{D}_O\frac{\partial\widetilde{Y}_O}{\partial\tilde{x}}\right)+\frac{\partial}{\partial\tilde{y}}\left(\tilde{\rho}_g\widetilde{D}_O\frac{\partial\widetilde{Y}_O}{\partial\tilde{y}}\right)-\nu_O\tilde{W}_O\tilde{\omega}_g \tag{6}$$

$$\tilde{P}=\tilde{\rho}_g\tilde{R}\tilde{T}_g \tag{7}$$

where

$$\tilde{\omega}_g=\tilde{B}_g\tilde{T}_g^{\beta}\left(\frac{\tilde{\rho}_g\widetilde{Y}_F}{\tilde{W}_F}\right)^{n_F}\left(\frac{\tilde{\rho}_g\widetilde{Y}_O}{\tilde{W}_O}\right)^{n_O}\exp\left(\frac{-\tilde{E}_g}{\tilde{R}_u\widetilde{T}_g}\right) \tag{8}$$

solid phase:

$$\tilde{\rho}_s\tilde{c}_{P,s}\frac{\partial\widetilde{T}_s}{\partial\tilde{t}}=\frac{\partial}{\partial\tilde{y}}\left(\tilde{\lambda}_s\frac{\partial\widetilde{T}_s}{\partial\tilde{y}}\right) \tag{9}$$

Boundary conditions in the gas phase are

at $\tilde{y}=0$

$$\tilde{u}=\tilde{v}=0,\quad -\tilde{\lambda}_g\frac{\partial\widetilde{T}_g}{\partial\tilde{y}}+\tilde{\lambda}_s\frac{\partial\widetilde{T}_s}{\partial\tilde{y}}=\tilde{W}_F\tilde{\omega}_{cat},$$
$$\tilde{\rho}_g\tilde{D}_F\partial\widetilde{Y}_F/\partial\tilde{y}=\tilde{W}_F\tilde{\omega}_{cat},\quad \tilde{\rho}_g\widetilde{D}_O\partial\widetilde{Y}_O/\partial\tilde{y}=\nu_O\tilde{W}_O\tilde{\omega}_{cat} \tag{10}$$

as $\tilde{y}\to\infty$

$$\tilde{u}\to\tilde{\gamma}\tilde{x},\quad \tilde{v}\to-\tilde{\gamma}\tilde{y},\quad \tilde{\rho}_g\to\tilde{\rho}_\infty,\quad \widetilde{T}_g\to\widetilde{T}_\infty,$$
$$\widetilde{Y}_F\to\widetilde{Y}_{F,\infty},\quad \widetilde{Y}_O\to\widetilde{Y}_{O,\infty},\quad \widetilde{Y}_O\to\widetilde{Y}_{O,\infty} \tag{11}$$

The initial condition of temperature in the solid phase is equal to $\widetilde{T}_L$ uniformly, where $\widetilde{T}_L$ is greater than $\widetilde{T}_\infty$. To avoid a temperature jump at the lower surface of plate for $t>0$, the boundary condition of temperature there is given by the initial value, i.e.,

$$\widetilde{T}_s=\widetilde{T}_L\quad\text{at }\tilde{y}=-\tilde{L} \tag{12}$$

Physically, the process of chemical reactions in the gas phase is much faster than the process of heat conduction in the solid plate. Therefore, the influence of temperature on the ignition delay is the initial temperature of solid plate instead of the temperature at the lower surface of plate. The initial conditions in the gas phase are provided by the steady solutions of isothermal stagnation-point flows at $\widetilde{T}_g=\widetilde{T}_\infty$.

According to the Arrhenius-type formula, the rate of catalytic reactions at the interfacial surface between the gas and solid phase is given by

$$\tilde{\omega}_{cat}=\tilde{B}_{cat}\widetilde{Y}_F\widetilde{Y}_O\exp\left(-\tilde{E}_{cat}/\tilde{R}_u\widetilde{T}\right) \tag{13}$$

The magnitude of $\tilde{\omega}_{cat}$ is equal to zero in the non-catalytic limit. In the strongly catalytic limit, the ignition in the gas phase is expected to be diffusionally controlled. In particular, the boundary conditions of concentrations

of species in this limit become $\widetilde{Y}_F = 0$ and $\widetilde{Y}_O = \widetilde{Y}_{O,\infty} - \sigma\widetilde{Y}_{F,\infty}$ for fuel-lean cases.

The non-dimensional variables are defined as follows:

$$x = \tilde{x}/\tilde{l}_t,\ y = \tilde{y}/\tilde{l}_t,\ y_s = \tilde{y}/\tilde{L},\ t = \tilde{s}_f\tilde{t}/\tilde{l}_t,\ \rho_g = \tilde{\rho}_g/\tilde{\rho}_\infty,$$
$$\rho_s = \tilde{\rho}_s/\tilde{\rho}_\infty,\ u = \tilde{u}/\tilde{s}_f,\ v = \tilde{v}/\tilde{s}_f,\ P = \tilde{P}/\tilde{P}_\infty,$$
$$T_g = \widetilde{T}_g/\widetilde{T}_\infty,\ T_s = \widetilde{T}_s/\widetilde{T}_\infty,\ Y_F = \widetilde{Y}_F,\ Y_O = \widetilde{Y}_O/\sigma,$$
$$\mu = \tilde{\mu}/\tilde{\mu}_\infty,\ \lambda_g = \tilde{\lambda}_g/\tilde{\lambda}_\infty,\ \lambda_s = \tilde{\lambda}_s/\tilde{\lambda}_\infty,\ D_i = \widetilde{D}_i/\widetilde{D}_{i,\infty},$$
$$c_{P,s} = \tilde{c}_{P,s}/\tilde{c}_{P,g},\ q = \tilde{q}/\tilde{c}_{P,g}\widetilde{T}_\infty,\ \theta_g = \tilde{E}_g/\hat{R}_u\widetilde{T}_\infty,$$
$$a_P = \tilde{P}_\infty/\tilde{\rho}_\infty\tilde{s}_f^2,\ Pr = \tilde{c}_{P,g}\tilde{\mu}_\infty/\tilde{\lambda}_\infty,\ Le_i = \tilde{\lambda}_\infty/\tilde{\rho}_\infty\tilde{c}_{P,g}\widetilde{D}_{i,\infty} \tag{14}$$

where $\tilde{l}_t = \tilde{\lambda}_\infty/\tilde{\rho}_\infty\tilde{c}_{P,g}\tilde{s}_f$ and $\sigma = \nu_O\tilde{W}_O/\tilde{W}_F$.

In terms of the above non-dimensional variables, the problem of interest becomes

gas phase:

$$\frac{\partial\rho_g}{\partial t} + \frac{\partial(\rho_g u)}{\partial x} + \frac{\partial(\rho_g v)}{\partial y} = 0 \tag{15}$$

$$\rho_g\left(\frac{\partial u}{\partial t} + u\frac{\partial u}{\partial x} + v\frac{\partial u}{\partial y}\right) = -a_P\frac{\partial P}{\partial x} + Pr\left\{\frac{\partial}{\partial y}\left[\mu\left(\frac{\partial u}{\partial y} + \frac{\partial v}{\partial x}\right)\right] + \frac{\partial}{\partial x}\left(2\mu\frac{\partial u}{\partial x}\right) - \frac{\partial}{\partial x}\left[\frac{2}{3}\mu\left(\frac{\partial u}{\partial x} + \frac{\partial v}{\partial y}\right)\right]\right\} \tag{16}$$

$$\rho_g\left(\frac{\partial v}{\partial t} + u\frac{\partial v}{\partial x} + v\frac{\partial v}{\partial y}\right) = -a_P\frac{\partial P}{\partial y} + Pr\left\{\frac{\partial}{\partial x}\left[\mu\left(\frac{\partial u}{\partial y} + \frac{\partial v}{\partial x}\right)\right] + \frac{\partial}{\partial y}\left(2\mu\frac{\partial v}{\partial y}\right) - \frac{\partial}{\partial y}\left[\frac{2}{3}\mu\left(\frac{\partial u}{\partial x} + \frac{\partial v}{\partial y}\right)\right]\right\} \tag{17}$$

$$\rho_g\left(\frac{\partial T_g}{\partial t} + u\frac{\partial T_g}{\partial x} + v\frac{\partial T_g}{\partial y}\right) = \frac{\partial}{\partial x}\left(\lambda_g\frac{\partial T_g}{\partial x}\right) + \frac{\partial}{\partial y}\left(\lambda_g\frac{\partial T_g}{\partial y}\right) + q\omega_g \tag{18}$$

$$\rho_g\left(\frac{\partial Y_i}{\partial t} + u\frac{\partial Y_i}{\partial x} + v\frac{\partial Y_i}{\partial y}\right) = Le_i^{-1}\left[\frac{\partial}{\partial x}\left(\rho_g D_i\frac{\partial Y_i}{\partial x}\right) + \frac{\partial}{\partial y}\left(\rho_g D_i\frac{\partial Y_i}{\partial y}\right)\right] - \omega_g, \quad i = F, O \tag{19}$$

$$\rho_g T_g = 1 \tag{20}$$

solid phase:

$$\frac{\partial T_s}{\partial t} = a_s\frac{\partial^2 T_s}{\partial y_s^2} \tag{21}$$

where $a_s = a_L^2\alpha_s$ and $\omega_g = B_g T_g^{\beta-n} Y_F^{n_F} Y_O^{n_O}\exp(-\theta_g/T_g)$ with $a_L = \tilde{l}_t/\tilde{L}$, $\alpha_s = \lambda_s/\rho_s c_{P,s}$, $B_g = (\tilde{B}_g\nu_O^{n_O}\tilde{\lambda}_\infty)/(\tilde{c}_{P,g}\tilde{\rho}_\infty^2\tilde{s}_f^2\times \tilde{W}_F^{n-1}\widetilde{T}_\infty^{n-\beta})(\tilde{P}_\infty/\tilde{R})^n$ and $n = n_F + n_O$. The boundary conditions Eqs. (10)–(12) become

at $y = 0$

$$u = v = 0, \quad -\lambda_g\frac{\partial T_g}{\partial y} + a_L\lambda_s\frac{\partial T_s}{\partial y_s} = q\omega_{cat},$$
$$\rho_g D_F\partial Y_F/\partial y = Le_F\omega_{cat}, \quad \rho_g D_O\partial Y_O/\partial y = Le_O\omega_{cat} \tag{22}$$

as $y \to \infty$

$$u \to \gamma x, \quad v \to -\gamma y, \quad \rho_g \to 1, \quad T_g \to 1,$$
$$Y_F \to Y_{F,\infty}, \quad Y_O \to Y_{O,\infty} \tag{23}$$

where $\gamma = \tilde{\lambda}_\infty\tilde{\gamma}/\tilde{\rho}_\infty\tilde{c}_{P,g}\tilde{s}_f^2$

at $y_s = -1, \quad T_s = T_L$ (24)

The rate of catalytic reactions at the wall becomes

$$\omega_{cat} = B_{cat}Y_F Y_O\exp(-\theta_{cat}/T) \text{ at } y = 0 \tag{25}$$

where $B_{cat} = \nu_O\tilde{W}_O\tilde{B}_{cat}/\tilde{\rho}_\infty\tilde{s}_f$ and $\theta_{cat} = \tilde{E}_{cat}/\tilde{R}_u\widetilde{T}_\infty$.

For the problem of interest, we have the following similar solutions in the gas phase

$$\rho_g = \rho_g(y,t), \quad u = xF(y,t), \quad v = v(y,t), \quad T_g = T_g(y,t),$$
$$Y_i = Y_i(y,t), \quad P = -\gamma^2x^2/2a_P + H(y,t),$$
$$\mu = \mu(T) = \mu(y,t), \quad \lambda_g = \lambda_g(T) = \lambda_g(y,t),$$
$$D_i = D_i(T) = D_i(y,t) \tag{26}$$

Substituting the above similar solutions, we have

$$\frac{\partial\rho_g}{\partial t} + \frac{\partial(\rho_g v)}{\partial y} + \rho F = 0 \tag{27}$$

$$\rho_g\left(\frac{\partial F}{\partial t} + v\frac{\partial F}{\partial y}\right) = -\rho_g F^2 + \gamma^2 + Pr\frac{\partial}{\partial y}\left(\mu\frac{\partial F}{\partial y}\right) \tag{28}$$

$$\rho_g\left(\frac{\partial v}{\partial t} + v\frac{\partial v}{\partial y}\right) = -\frac{\partial H}{\partial y} + Pr\left\{\mu\frac{\partial F}{\partial y} + 2\frac{\partial}{\partial y}\left(\mu\frac{\partial v}{\partial y}\right) - \frac{2}{3}\frac{\partial}{\partial y}\left[\mu\left(F + \frac{\partial v}{\partial y}\right)\right]\right\} \tag{29}$$

$$\rho_g\left(\frac{\partial T_g}{\partial t} + v\frac{\partial T_g}{\partial y}\right) = \frac{\partial}{\partial y}\left(\lambda_g\frac{\partial T_g}{\partial y}\right) + q\omega_g \tag{30}$$

$$\rho_g\left(\frac{\partial Y_i}{\partial t} + v\frac{\partial Y_i}{\partial y}\right) = Le_i^{-1}\frac{\partial}{\partial y}\left(\rho_g D_i\frac{\partial Y_i}{\partial y}\right) - \omega_g \tag{31}$$

according to Eqs. (15)–(19).

3. Criteria of ignition

Basically, there are two types of ignition criteria for the problem of interest, i.e., the zero-gradient criteria ($\partial T_g/\partial y = 0$ and $\partial\omega_g/\partial y = 0$ at wall) and the criteria of thermal runaway ($\partial^2 T_{g,max}/\partial t^2 = 0$ and $\partial^2\omega_{g,max}/\partial t^2 = 0$).

The validity of these ignition criteria for the interest of problem will be discussed later.

4. Numerical method

The method of lines [26] is adopted to solve Eqs. (27)–(31). All spatial derivatives are discretized according to a power law [27] whereas the time derivative remains continuous. Thus the partial differential equation is reduced to a system of coupled non-linear ordinary differential equations that is readily treated by the fourth-order accurate Runge–Kutta–Fehlberg scheme with a local integration error equal to 10^{-5}. The infinite domain in the gas phase is truncated from $y = 0$ to $y = 45$ in the computation. The results reveal that the numerical solutions are not influenced as the computational domain further increases. The numbers of grid points are 450 and 10 in the gas phase and in the solid phase, respectively. The time step is 10^{-3}. For the present grid system and time step, the maximum relative error of ignition delay is estimated to be 3%.

The premixed butane-air flow with a equivalence ratio equal to 0.8 is considered in the present work. The input parameters concerned with the global one-step chemical reaction mechanism of butane-air are available [28]. The other system parameters are $\tilde{P} = 1$ atm, $\tilde{c}_{P,g} = 1.05 \times 10^{-3}$ kJ/g K, $T_\infty = 1.0$, $\tilde{l}_t = 0.05$ mm and $\theta_{cat} = 13.33$. According to the process of conduction heat transfer in the solid plate described by Eq. (21), an increase in a_s ($= a_L^2 \alpha_s$ with $a_L = \tilde{l}_t/\tilde{L}$) can be achieved by either increasing the thermal diffusivity of solid plate or decreasing the thickness of solid plates. For simplicity, the thickness of solid plate is fixed in this work ($\tilde{L} = 5$ cm); thereby the value of a_L is equal to 10^{-3}. Physically, a marked variation in the thermal diffusivities of solid materials is found [29,30]. Based on the non-dimensional definition of thermal diffusivity in this work, the magnitudes of α_s are 3.789, 0.283 and 0.002 for Cu, Fe and Al_2O_3, respectively. According to Eq. (21), the following non-dimensional results are also valid if a_s ($= a_L^2 \alpha_s$) is fixed even though the variation of thermal diffusivity and thickness of solid plate occurs.

5. Results and discussion

For the purpose of qualitative analysis in this work, the rate of catalytic surface reactions is varied just by modifying the magnitude of frequency factor of catalytic surface reactions (B_{cat}) [17]. The rate of catalytic reactions is proportional to the magnitude of B_{cat}.

5.1. Ignition in the non-catalytic limit

Plot of the magnitude of ignition delay (t_{ig}^o) versus the temperature of lower surface of plate (T_L) in the non-catalytic limit ($B_{cat} = 0$) according to four types of ignition criteria is shown in Fig. 2. The qualitative results of ignition delay are basically the same no matter what ignition criterion is adopted. The values of t_{ig}^o predicted by the thermal runaway criteria ($\partial^2 T_{g,max}/\partial t^2 = 0$ and $\partial^2 \omega_{g,max}/\partial t^2 = 0$) are invariably greater than those predicted by the zero-gradient criteria ($\partial T_g/\partial y = 0$ and $\partial \omega_g/\partial y = 0$ at wall), as physically expected. Although the quantitative discrepancy of ignition delay decreases gradually with T_L according to Fig. 2, the relative difference in ignition delay almost keeps a constant.

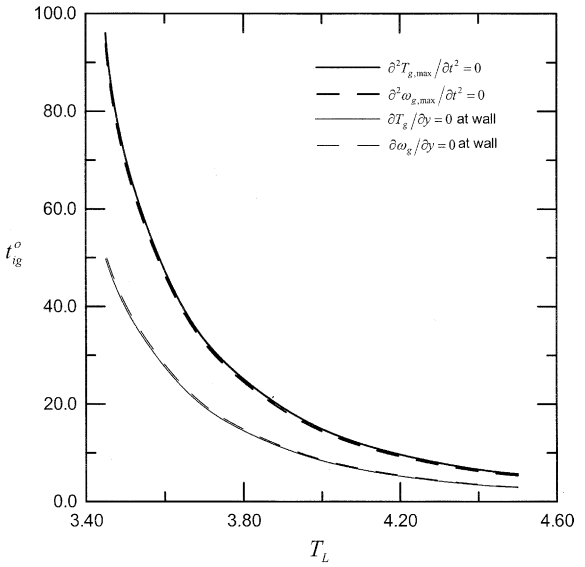

Fig. 2. t_{ig}^o versus T_L according to various ignition criteria ($B_{cat} = 0$, $\alpha_s = 0.283$, $\gamma = 0.01$, $Le_F = Le_O = 1.0$ and $Pr = 0.7$).

In the non-catalytic limit, there is a certain value of the initial temperature of solid plate below which the gaseous premixture cannot be ignited no matter how long the ignition process proceeds. This critical temperature is termed as the minimum ignition temperature without any catalytic reaction ($T_{L,min}^o$). The magnitudes of $T_{L,min}^o$ versus the flow strain rate (γ) according to the criteria of $\partial T_g/\partial y = 0$ at wall and $\partial^2 T_{g,max}/\partial t^2 = 0$ are presented in Fig. 3. As a boundary condition in the steady model, the dependence of $T_{L,min}^o$ on system parameters has been analyzed according to the criterion of $\partial T_g/\partial y = 0$ at wall [2]. The value of $T_{L,min}^o$ increases with γ, as expected physically. It is interesting to note that the region of no ignition obtained by the thermal runaway criterion ($\partial^2 T_{g,max}/\partial t^2 = 0$) is greater than that obtained by the zero-gradient criterion ($\partial T_g/\partial y = 0$). This fact implies that the ignition is eventually not achieved in the region between two curves in Fig. 3 even though the criterion of $\partial T_g/\partial y = 0$ at wall is satisfied in this region. In other words, the zero-gradient ignition criterion [2] is

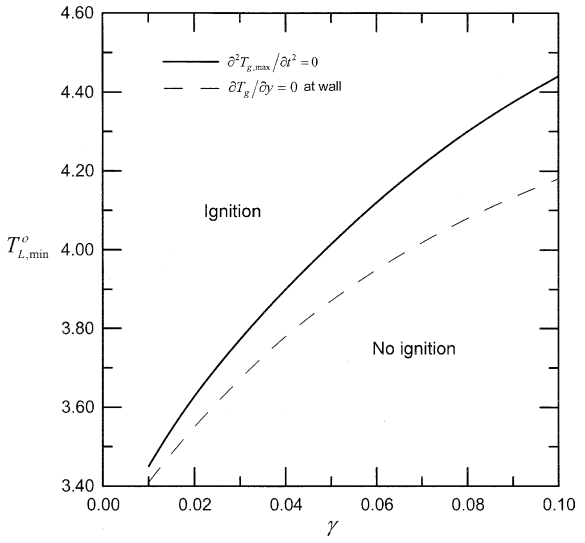

Fig. 3. $T^{o}_{L,\min}$ versus γ according to $\partial^2 T_{g,\max}/\partial t^2 = 0$ and $\partial T_g/\partial y = 0$ at wall ($B_{cat} = 0$, $\alpha_s = 0.283$, $T_L = 4.5$, $Le_F = Le_O = 1.0$ and $Pr = 0.7$).

just a necessary condition for thermal ignition. According to Fig. 3, this region increases with γ.

The ignition delay (t^{o}_{ig}) as a function of the thermal diffusivity of solid plate (α_s) is shown in Fig. 4. Besides the quantitative variation, as shown in Fig. 4, the qualitative behavior of ignition delay determined by the thermal runaway criterion is different from that determined by the zero-gradient criterion. The ignition delay

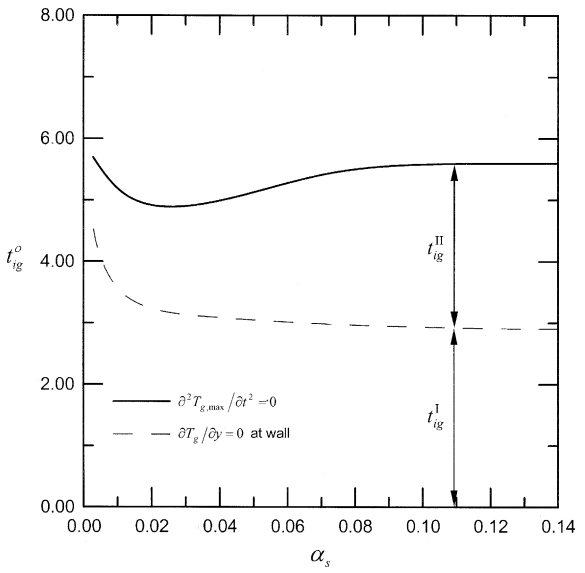

Fig. 4. Results of t^{o}_{ig}, t^{I}_{ig} and t^{II}_{ig} versus α_s according to $\partial^2 T_{g,\max}/\partial t^2 = 0$ and $\partial T_g/\partial y = 0$ at wall ($B_{cat} = 0$, $\gamma = 0.01$, $T_L = 4.5$, $Le_F = Le_O = 1.0$ and $Pr = 0.7$).

decreases monotonically with α_s according to the zero-gradient criterion. However, the ignition delay according to the thermal runaway criterion decreases initially with α_s, and then increases with it after the magnitude of α_s is greater than a critical value ($\alpha_{s,c} = 0.0262$). The ignition delay is minimum at $\alpha_s = \alpha_{s,c}$.

For the convenience of interpretation, the period of ignition delay is divided into two stages. The thermal energy is initially transferred from the solid phase to the gas phase when the process of ignition starts for the problem of interest. This stage is called as the first stage of ignition delay (t^{I}_{ig}) at which the internal energy in the solid phase decreases. If the ignition process continues, the thermal energy will be eventually transferred from the gas phase to the solid phase when the temperature of gaseous mixture is greater than that of solid plate due to sufficiently rapid chemical reactions. This stage is called as the second stage of ignition delay (t^{II}_{ig}) at which the internal energy in the solid phase increases. In the non-catalytic limit, the value of t^{o}_{ig} obtained by the criterion of $\partial T_g/\partial y = 0$ at wall is exactly equal to the value of t^{I}_{ig} because the achievement of ignition is considered as the adiabaticity condition is satisfied. However, the magnitude of t^{o}_{ig} is the sum of t^{I}_{ig} and t^{II}_{ig} for the thermal runaway criterion, as shown in Fig. 4.

Based on the above discussion, the magnitude of t^{I}_{ig} is physically expected to decrease with α_s due to the enhanced heat transfer from the hot solid plate to the cold gaseous mixture. As a result, the ignition delay according to the criterion of $\partial T_g/\partial y = 0$ at wall decreases invariably with α_s. The ignition delay t^{II}_{ig} is not taken into account for this criterion because the ignition delay is obtained immediately when the gas-phase temperature near the wall increases up to the temperature of upper surface of plate. Similarly, the rate of heat transfer from the gaseous mixture to the solid plate also increases with α_s during the second stage of ignition after the gas-phase temperature near the wall exceeds the temperature of upper surface of plate. The magnitude of t^{II}_{ig} is expected to increase with α_s due to an increase in the rate of heat loss of gaseous mixture. Obviously, there is a qualitative difference in the influence of α_s on t^{I}_{ig} and t^{II}_{ig}. This fact implies that a minimum ignition delay exists at a critical value of α_s for the thermal runaway criterion because the corresponding ignition delay is the sum of t^{I}_{ig} and t^{II}_{ig}, as shown in Fig. 4. Physically, the ignition phenomena will be modified if the catalytic reaction is involved.

Figs. 5 and 6 show the interfacial temperature between the gas phase and the solid phase (T_{int}) as a function of time for $\alpha_s < \alpha_{s,c}$ and $\alpha_s > \alpha_{s,c}$, respectively. Because a temperature jump initially appears at the interface, the magnitude of T_{int} presented in Figs. 5 and 6 is the temperature of gaseous mixture just above the interface. The period of heat loss from the gas phase to the solid phase is indicated. Based on the thermal runaway criterion, the process of heat loss in the gas phase is

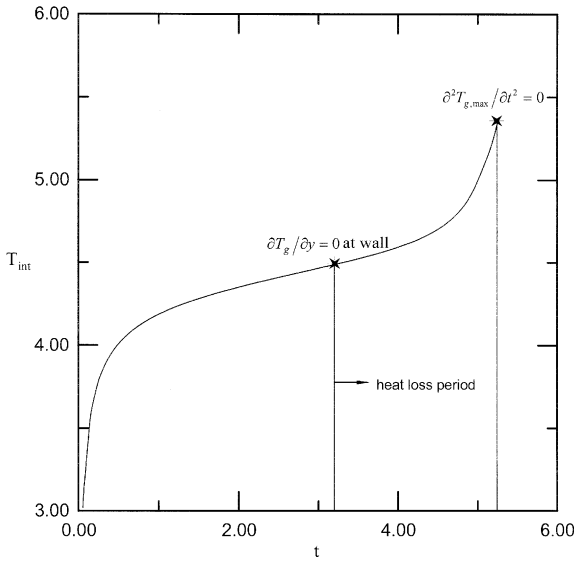

Fig. 5. Result of T_{int} as a function of time for $\alpha_s < \alpha_{s,c}$ ($\alpha_s = 0.0177$, $B_{cat} = 0$, $\gamma = 0.01$, $T_L = 4.5$, $Le_F = Le_O = 1.0$ and $Pr = 0.7$).

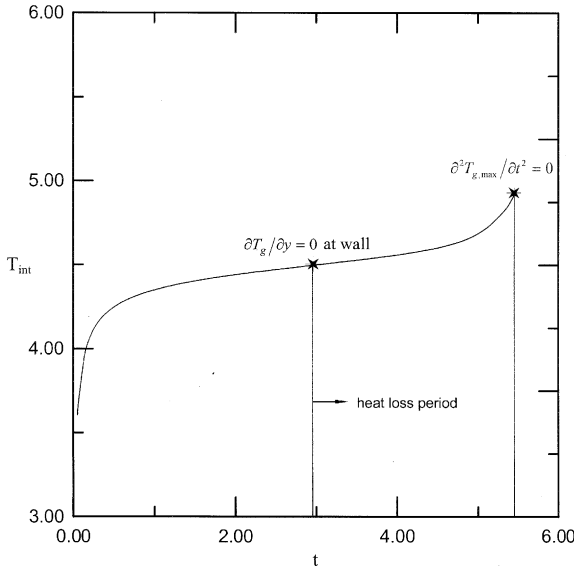

Fig. 6. Result of T_{int} as a function of time for $\alpha_s > \alpha_{s,c}$ ($\alpha_s = 0.071$, $B_{cat} = 0$, $\gamma = 0.01$, $T_L = 4.5$, $Le_F = Le_O = 1.0$ and $Pr = 0.7$).

inevitable for any α_s. As a result, both the ignition delay and the minimum ignition temperature are underestimated if the zero-gradient criterion is used.

According to the above discussion, the correct ignition delay is determined by the thermal runaway criterion instead of the zero-gradient criterion. The same conclusion was obtained for the ignition delay of non-premixed stagnation-point flows in the previous paper [25].

5.2. Ignition with the variation of rate of catalytic reactions

The results of ignition delay versus the rate of catalytic reactions (B_{cat}) for $\alpha_s = 0.283$ according to various ignition criteria are illustrated in Fig. 7. The same ignition delay is predicted by either $\partial^2 T_{g,max}/\partial t^2 = 0$ or $\partial^2 \omega_{g,max}/\partial t^2 = 0$. However, in contrast to the results in Fig. 2, the ignition delay obtained by $\partial T_g/\partial y = 0$ is different from that obtained by $\partial \omega_g/\partial y = 0$ even in the qualitative way. According to Fig. 7, the quantitative difference in the ignition delay obtained by two zero-gradient criteria increases substantially with B_{cat}.

According to the criterion of $\partial^2 T_{g,max}/\partial t^2 = 0$, the ignition delay ($t_{ig}$) as a function of B_{cat} for varied α_s is shown in Fig. 8. As shown in Fig. 8, the ignition delay increases monotonically with B_{cat} for great α_s ($\alpha_s = 0.071$). On the contrary, the ignition delay decreases monotonically with α_s for small α_s ($\alpha_s = 0.000353$). For an intermediate value of α_s, a minimum value of ignition delay ($t_{ig,min}$) is observed at a critical value of B_{cat} ($B_{cat,c}$). The ignition delay decreases and increases with B_{cat} for $B_{cat} < B_{cat,c}$ and $B_{cat} > B_{cat,c}$, respectively. Results of t_{ig}^{I} and t_{ig}^{II} for $\alpha_s = 0.071$ and 0.000353 are shown in Figs. 9 and 10, respectively. The magnitudes of t_{ig}^{I} in Figs. 9 and 10 decrease with B_{cat}. The temperature of gaseous mixture increases more rapidly for a greater rate of catalytic reactions at the upper surface of the plate. Consequently, the duration of heat transfer from the solid

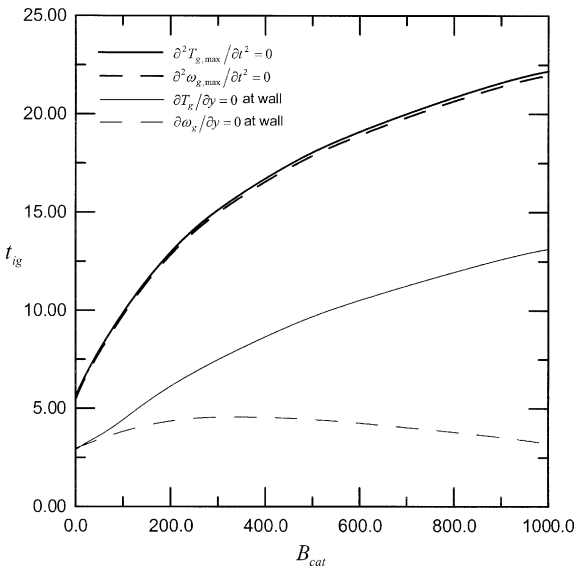

Fig. 7. t_{ig} versus B_{cat} according to various ignition criteria ($\alpha_s = 0.283$, $\gamma = 0.01$, $T_L = 4.5$, $Le_F = Le_O = 1.0$ and $Pr = 0.7$).

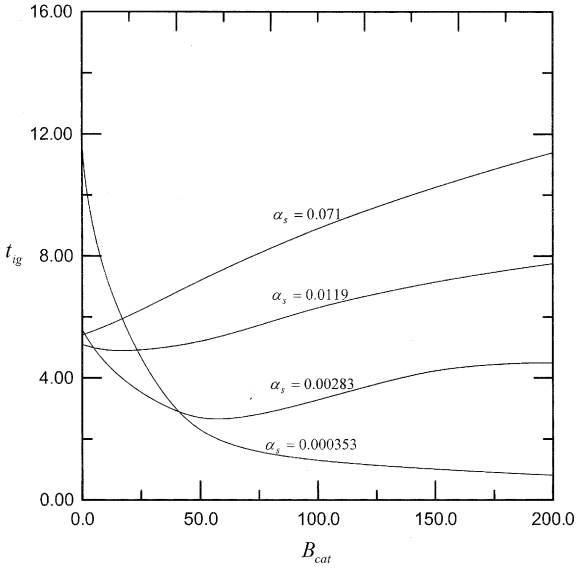

Fig. 8. t_{ig} versus B_{cat} for varied α_s according to $\partial^2 T_{g,max}/\partial t^2 = 0$ ($\gamma = 0.01$, $T_L = 4.5$, $Le_F = Le_O = 1.0$ and $Pr = 0.7$).

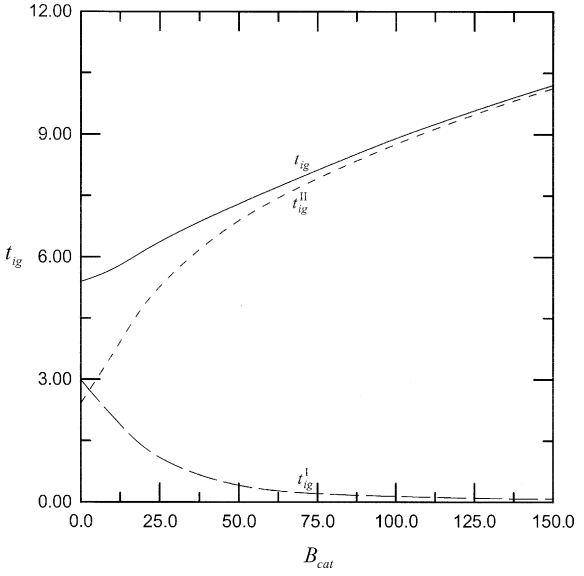

Fig. 9. Results of t_{ig}, t_{ig}^{I} and t_{ig}^{II} versus B_{cat} according to $\partial^2 T_{g,max}/\partial t^2 = 0$ ($\alpha_s = 0.071$, $\gamma = 0.01$, $T_L = 4.5$, $Le_F = Le_O = 1.0$ and $Pr = 0.7$).

phase to the gas phase becomes shorter for greater B_{cat}. This fact indicates that the ignition delay in the first stage (t_{ig}^{I}) decreases with B_{cat}. As shown in Fig. 9, the magnitude of t_{ig}^{II} increases substantially with B_{cat}. The total ignition delay (t_{ig}) is almost equal to the value of t_{ig}^{II} for great B_{cat}. Physically, the rate of heat loss in the gas phase increases with the thermal diffusivity of solid plate when the ignition proceeds in the second stage. For great

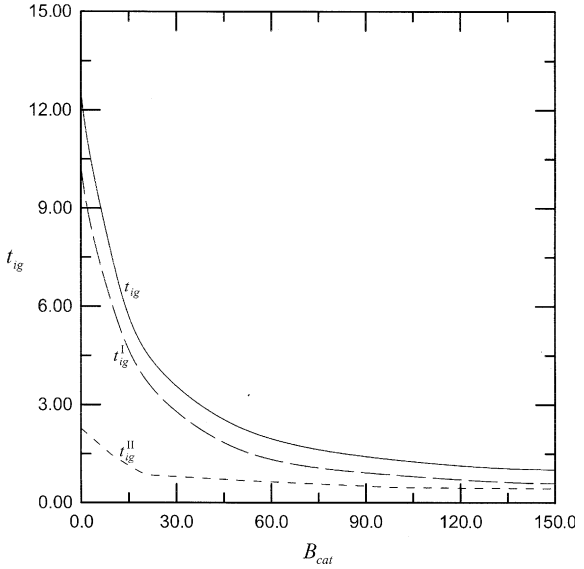

Fig. 10. Results of t_{ig}, t_{ig}^{I} and t_{ig}^{II} versus B_{cat} according to $\partial^2 T_{g,max}/\partial t^2 = 0$ ($\alpha_s = 0.000353$, $\gamma = 0.01$, $T_L = 4.5$, $Le_F = Le_O = 1.0$ and $Pr = 0.7$).

$\alpha_s (= 0.071)$, the effect of heat loss in the gas phase on ignition delay is greater than that of heat gain from the catalytic reaction on it. Physically, the ignition delay is conductively controlled for great α_s. This fact is significant to determine the ignition delay for great α_s. According to Fig. 9, the value of t_{ig} increases with B_{cat} even though the ignition delay in the first stage decreases with B_{cat}. For small α_s (Fig. 10), the influence of heat gain from the catalytic reaction on ignition delay is greater than that of heat loss in the gas phase on it. As a result, both of t_{ig}^{II} and t_{ig} decrease with B_{cat}. Physically, the ignition delay for small α_s becomes catalytically controlled.

For intermediate α_s ($= 0.00283$ in Fig. 8), the ignition delay decreases initially with B_{cat} and then increases with it after B_{cat} reaches a certain critical value ($B_{cat,c}$). The ignition delay is minimum at $B_{cat} = B_{cat,c}$. According to Fig. 8, the magnitudes of $B_{cat,c}$ and $t_{ig,min}$ decrease and increase with α_s, respectively. Physically, the influence of heat gain due to the catalytic reaction on ignition delay is greater than that of heat loss due to the solid plate on it for $B_{cat} < B_{cat,c}$, and vice versa for $B_{cat} > B_{cat,c}$. The processes of ignition here are controlled catalytically and conductively for $B_{cat} < B_{cat,c}$ and $B_{cat} > B_{cat,c}$, respectively.

5.3. Critical rate of catalytic reactions at ignition

According to the thermal runaway criterion ($\partial^2 T_{g,max}/\partial t^2 = 0$), the results of the critical rate of catalytic reactions at ignition ($B_{cat,ig}$) versus T_L for varied α_s are

shown in Figs. 11–13, respectively. Conventionally, the critical rates of catalytic reactions at ignition in previous works [17] were determined by the zero-gradient criterion ($\partial T_g/\partial y = 0$ at wall) according to a steady model instead of the thermal runaway criterion ($\partial^2 T_{g,max}/\partial t^2 = 0$) according to a transient model. Obviously, the critical rates of catalytic reactions at ignition obtained here are more realistic than those obtained before from a viewpoint of flame propagation. For great, α_s, the value

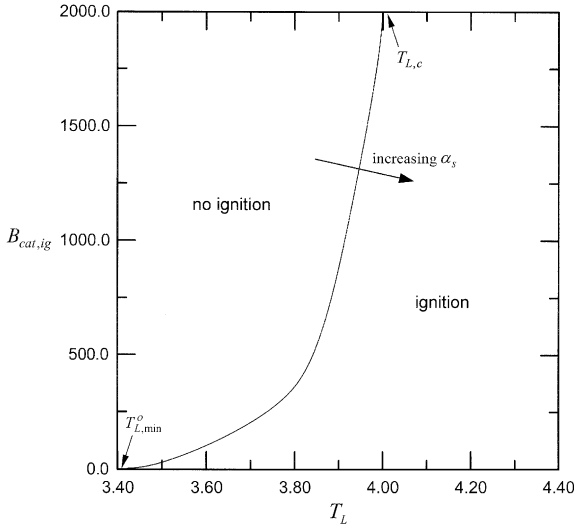

Fig. 11. $B_{cat,ig}$ versus T_L according to $\partial^2 T_{g,max}/\partial t^2 = 0$ ($\alpha_s = 0.071$, $\gamma = 0.01$, $Le_F = Le_O = 1.0$ and $Pr = 0.7$).

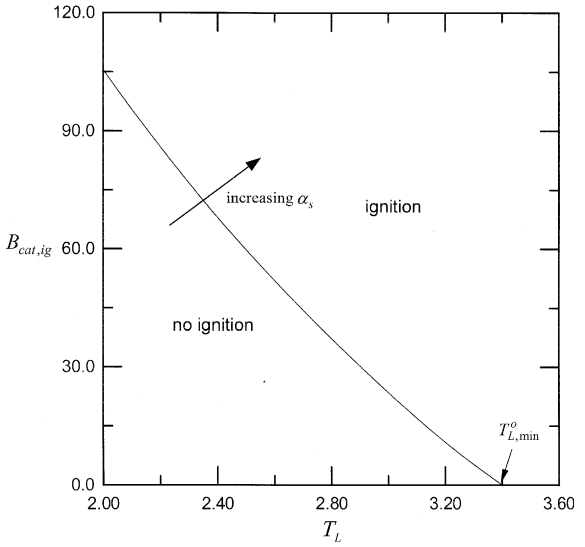

Fig. 12. $B_{cat,ig}$ versus T_L according to $\partial^2 T_{g,max}/\partial t^2 = 0$ ($\alpha_s = 0.000353$, $\gamma = 0.01$, $Le_F = Le_O = 1.0$ and $Pr = 0.7$).

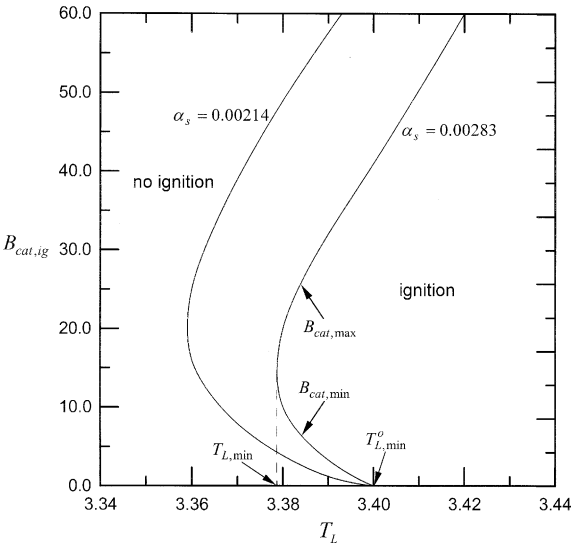

Fig. 13. $B_{cat,ig}$ versus T_L for $\alpha_s = 0.00214$ and 0.00283 according to $\partial^2 T_{g,max}/\partial t^2 = 0$ ($\gamma = 0.01$, $Le_F = Le_O = 1.0$ and $Pr = 0.7$).

of $B_{cat,ig}$ increases monotonically with T_L, as shown in Fig. 11 ($\alpha_s = 0.071$). The magnitude of $T^o_{L,min}$ is equal to 3.40. This fact implies that the ignition in the non-catalytic limit is invariably achieved if $T_L > T^o_{L,min}$. When the catalytic reactions are involved in the system, the ignition for fixed T_L exists only in the region between $B_{cat} = 0$ and $B_{cat} = B_{cat,max}$ even though T_L is greater than $T^o_{L,min}$ according to Fig. 11. As a result, the critical rate of catalytic reactions at ignition for great α_s is a maximum one ($B_{cat,max}$) above which the ignition can not be achieved. Physically, the catalytic reaction plays a negative role in ignition for great α_s. Similar to the results of ignition delay shown in Fig. 8, the critical rate of catalytic reactions at ignition is influenced mainly by the process of heat loss from the gas phase to the solid phase. The ignition is conductively controlled. According to Fig. 11, there is a critical value of T_L ($T_{L,c} = 4.11$) above which the ignition is eventually achieved no matter how rapidly the catalytic reactions proceed. The magnitude of $T_{L,c}$ here depends on α_s. Physically, the region of no ignition increases with α_s. Consequently, the value of $T_{L,c}$ is expected to increase with α_s.

For small α_s ($= 0.000353$), the ignition may be achieved with catalytic reactions even if $T_L < T^o_{L,min}$ ($= 3.40$), as shown in Fig. 12. This fact indicates that the catalytic reaction plays a positive role in ignition for small α_s. The ignition for small α_s is governed by the heat gain from the catalytic reactions. The ignition is catalytically controlled, as discussed previously. The critical rate of catalytic reactions at ignition here becomes a minimum one above which the ignition is achieved. Similar to the results in Fig. 11, the region of no ignition increases with α_s.

For intermediate α_s ($= 0.00214$ and 0.00283), the relationships between $B_{cat,ig}$ and T_L exhibit the C-shaped curves, as shown in Fig. 13. According to this figure, a minimum magnitude of T_L ($T_{L,min} = 3.378$) for $\alpha_s = 0.00283$ exists below which the ignition is not achieved. Obviously, the value of $T_{L,min}$ can be viewed as the minimum ignition temperature with catalytic reactions. The lack of ignition is observed if $T_L < T_{L,min}$. For $T^o_{L,min} > T_L > T_{L,min}$, the region of ignition is found between $B_{cat} = B_{cat,min}$ to $B_{cat} = B_{cat,max}$. The upper and lower branches of C-shaped ignition curves are dominated by the process of heat loss to the solid plate and the process of heat gain from the catalytic reaction, respectively. For fixed T_L ($T^o_{L,min} > T_L > T_{L,min}$), with increasing B_{cat} the transition from the catalytically to the conductively controlled ignition occurs. For $T_L > T^o_{L,min}$, the region of ignition exists from $B_{cat} = 0$ (non-catalytic limit) to $B_{cat} = B_{cat,max}$. The entire region of ignition is conductively controlled.

The value of $T_{L,min}$ increases with α_s according to Fig. 13. The upper limit of $T_{L,min}$ is physically expected to be $T^o_{L,min}$ when the value of α_s continuously increases up to a certain critical value ($\alpha^u_{s,c}$). Obviously, this critical magnitude of is an upper limit of intermediate α_s. The lower branch of C-shaped ignition curves (or catalytically controlled ignition mechanism) is absent at $\alpha_s = \alpha^u_{s,c}$; thereby the entire region of ignition becomes conductively controlled. The lower limit of α_s ($\alpha^l_{s,c}$) is corresponding to the condition of the vanishment of upper branch ($B_{cat,max}$) as the value of α_s decreases down to a certain small value ($\alpha^l_{s,c}$). The entire region of ignition becomes catalytically controlled at $\alpha_s = \alpha^l_{s,c}$. According to these two critical values of α_s, the C-shaped ignition curves are observed for $\alpha^u_{s,c} > \alpha_s > \alpha^l_{s,c}$.

6. Concluding remarks

The influence of catalytic reactions on the ignition of premixed stagnation-point flows over a solid plate with a finite thickness is analyzed numerically. The following conclusions are obtained.

(i) The thermal runaway criterion instead of the zero-gradient criterion is preferred to predict the ignition delay for the problem of interest even in the non-catalytic limit.

(ii) The ignition for small α_s is governed by the heat gain from the catalytic reactions. The effect of catalytic reactions on ignition is positive. The ignition is catalytically controlled. However, the ignition for great α_s is influenced mainly by the process of heat loss from the gaseous mixture to the solid plate. The effect of catalytic reactions on ignition is negative. The ignition becomes conductively controlled.

(iii) The magnitudes of ignition delay increase and decrease monotonically with the rate of catalytic reactions for great and small α_s, respectively. For intermediate α_s, there is a minimum ignition delay at $B_{cat} = B_{cat,c}$. The magnitudes of ignition delay decrease and increase with B_{cat} for $B_{cat} < B_{cat,c}$ (catalytically controlled ignition) and $B_{cat} > B_{cat,c}$ (conductively controlled ignition), respectively.

(iv) For great α_s ($\alpha_s > \alpha^u_{s,c}$), the critical rate of catalytic reactions at ignition is a maximum one below which the ignition is achieved. The value of $B_{cat,max}$ increases with T_L. There is a critical value of T_L ($T_{L,c}$) above which the values of $B_{cat,max}$ invariably approach infinity. The magnitude of $T_{L,c}$ increases with α_s. For small α_s ($\alpha_s < \alpha^l_{s,c}$), the critical rate of catalytic reactions at ignition is a minimum one above which the ignition is achieved. The value of $B_{cat,min}$ decreases with T_L. For intermediate α_s ($\alpha^u_{s,c} > \alpha_s > \alpha^l_{s,c}$), the C-shaped ignition curves are observed. The upper (conductively controlled) and lower (catalytically controlled) branches of C-shaped ignition curves indicate the values of $B_{cat,max}$ and $B_{cat,min}$, respectively. The region of ignition depends on T_L, $T^o_{L,min}$ and $T_{L,min}$. According to the C-shaped ignition curve, the lack of ignition is obtained if $T_L < T_{L,min}$. The magnitude of $T_{L,min}$ increases with α_s. For $T^o_{L,min} > T_L > T_{L,min}$, the region of ignition is confined between $B_{cat,min}$ to $B_{cat,max}$. As the rate of catalytic reactions increases for fixed T_L, the transition of ignition from the catalytically controlled to the conductively controlled mechanism is observed. For $T_L > T^o_{L,min}$, the region of conductively controlled ignition is from the non-catalytic limit to $B_{cat,max}$. The region of ignition decreases with α_s for any range of α_s according to the thermal runaway criterion.

Acknowledgement

This work was supported by the National Science Council, Taiwan, ROC under contract number NSC 89-2212-E-007-091.

References

[1] T. Niioka, F.A. Williams, Ignition of a reactive solid in a hot stagnation-point flow, Combust. Flame 29 (1977) 43–54.

[2] C.K. Law, On the stagnation-point ignition of a premixed combustible, Int. J. Heat Mass Transfer 21 (1978) 1363–1368.

[3] C.K. Law, H.K. Law, Thermal-ignition analysis in boundary-layer flows, J. Fluid Mech. 92 (1979) 97–108.

[4] C. Treviño, M. Sen, Effect of Prandtl number on boundary layer ignition, Combust. Flame 46 (1982) 211–212.

[5] C. Treviño, A.C. Fernandez-Pello, On the influence of the plate thickness on the boundary layer ignition for large activation energies, Combust. Flame 49 (1983) 91–100.
[6] M.M. Yan, L.D. Chen, G.M. Faeth, Analysis of ignition by a plane laminar thermal plume, Combust. Flame 58 (1984) 1–12.
[7] Y. Ju, T. Niioka, Ignition analysis of unpremixed reactants with chain mechanism in a supersonic mixing layer, AIAA J. 31 (1993) 863–868.
[8] M.C. Lin, W.J. Sheu, Theoretical criterion for ignition of a combustible gas flowing over a wedge, Combust. Sci. Tech. 99 (1994) 299–312.
[9] W.J. Sheu, M.C. Lin, Thermal ignition in buoyancy-driven boundary-layer flows along inclined hot plates, Int. J. Heat Mass Transfer 39 (1996) 2187–2190.
[10] W.J. Sheu, M.C. Lin, Ignition of non-premixed wall-bounded boundary-layer flows, Combust. Sci. Tech. 122 (1997) 231–255.
[11] W.J. Sheu, M.C. Lin, Ignition of accelerated boundary-layer flows under mixed convection, Combust. Sci. Tech. 130 (1997) 1–24.
[12] W.J. Sheu, M.C. Lin, Ignition of plane laminar premixed jets in a hot inert environment, Combust. Flame 112 (1998) 285–292.
[13] C. Treviño, Gas-phase ignition of premixed fuel by catalytic bodies in stagnation flow, Combust. Sci. Tech. 30 (1983) 213–229.
[14] C. Treviño, N. Peters, Gas-phase boundary layer ignition on a catalytic flat plate with heat loss, Combust. Flame 51 (1985) 39–49.
[15] W.J. Sheu, M.C. Lin, Gas-phase ignition of accelerated boundary-layer flows on strongly catalytic surfaces, Combust. Flame 103 (1995) 161–170.
[16] C. Treviño, F. Mendez, Ignition of catalytic reactions in a vertical wall immersed in a combustible gas, 26th Symposium (Int.) on Combustion, The Combustion Institute, Pittsburgh, 1996, pp. 1797–1804.
[17] W.J. Sheu, K.C. Chen, N.C. Liou, Critical rate of reactions at gas-phase ignition of non-premixed stagnation-point flows, Combust. Sci. Tech. 137 (1998) 101–120.
[18] W.J. Sheu, H.C. Shia, N.C. Liou, Ignition length of laminar combustible pipe flows, Combust. Sci. Tech. 140 (1998) 451–459.
[19] C. Treviño, J.C. Prince, J. Tejero, Catalytic ignition of dry carbon monoxide in a stagnation-point flow, Combust. Flame 119 (1999) 505–512.
[20] J. Mantzaras, P. Benz, An asymptotic and numerical investigation of homogeneous ignition in catalytically stabilized channel flow combustion, Combust. Flame 119 (1999) 455–472.
[21] C. Treviño, M. Sen, Transient phenomena in boundary layer ignition with finite plate thermal resistance, 18th Symposium (Int.) on Combustion, The Combustion Institute, Pittsburgh, 1981, pp. 1781–1789.
[22] A. Liñan, C. Treviño, Transient catalytic ignition on a flat plate with external energy flux, AIAA J. 23 (1985) 1716–1723.
[23] O. Deutschmann, R. Schmidt, F. Behrendt, J. Warnatz, Numerical modeling of catalytic ignition, 26th Symposium (Int.) on Combustion, The Combustion Institute, Pittsburgh, 1996, pp. 1747–1754.
[24] M. Rinnemo, O. Deutschmann, F. Behrendt, B. Kasemo, Experimental and numerical investigation of the catalytic ignition of mixtures of hydrogen and oxygen on platinum, Combust. Flame 111 (1997) 312–326.
[25] W.J. Sheu, C.J. Sun, Ignition delay of non-premixed stagnation-point flows, Int. J. Heat Mass Transfer 45 (2002) 3549–3558.
[26] J.I. Ramos, On some accurate finite-difference methods for laminar flame calculation, Int. J. Num. Meth. Fluids 4 (1984) 915–930.
[27] S.V. Patankar, in: Numerical Heat Transfer and Fluid Flow, Hemisphere, New York, 1980, pp. 90–96.
[28] C.K. Westbrook, F.L. Dryer, Simplified reaction mechanisms for the oxidation of hydrocarbon fuels in flames, Combust. Sci. Tech. 27 (1981) 31–43.
[29] F.P. Incropera, D.P. Dewitt, in: Fundamentals of Heat and Mass Transfer, John Wiley & Sons, New York, 1996, pp. 827–828.
[30] E.R. Parker, Material Data Book for Engineers and Scientists, McGraw-Hill, New York, 1967, pp. 262–230.